In vitro and biomechanical screening of polyethylene glycol and poly(trimethylene carbonate) block copolymers for annulus fibrosus repair

Rose G. Long,

Degree: BS

Telephone: 01 802 448 0917

Fax: 081 414 22 88

E-mail: rose.long@mssm.edu

Mailing Address:

Leni & Peter W. May Department of Orthopaedics, Icahn School of Medicine at Mount Sinai, New York, NY, 10029

Collaborative Research Partner Annulus Fibrosus Rupture Program of AO Foundation, Davos, Switzerland

Stijn G. Rotman,

Degree: BS

Telephone: 31 74 266 8899

Fax: 31 53 489 2155

E-mail: s.g.rotman@student.utwente.nl

Mailing Address: University of Twente, Department of Biomaterials Science and Technology, PO Box 217, 7500 AE Enschede, The Netherlands

This article has been accepted for publication and undergone full peer review but has not been through the copyediting, typesetting, pagination and proofreading process which may lead to differences between this version and the Version of Record. Please cite this article as doi: 10.1002/term.2356

Warren W. Hom,

Degree: MS

Telephone: 1-212-241-1045

Fax: 1-212-876-3168

E-mail: warren.hom@mssm.edu

Mailing Address: Leni & Peter W. May Department of Orthopaedics, Icahn School of Medicine at Mount Sinai, New York, NY

Dylan J. Assael,

Degree: BS

Telephone: 516-695-3484

Fax: n/a

E-mail: dylan.assael@icahn.mssm.edu

Mailing Address: Leni & Peter W. May Department of Orthopaedics, Icahn School of Medicine at Mount Sinai, New York, NY

Svenja Illien-Jünger,

Degree: PhD

Telephone: +1 212 241 1513

Fax: 1-212-876-3168

E-mail: Svenja.illien-junger@mssm.edu

Mailing Address: Leni & Peter W. May Department of Orthopaedics, Box 1188, Icahn School of Medicine at Mount Sinai, New York, NY, 10029

Dirk W. Grijpma,

Degree: PhD

Telephone: 31 53 489 2966

Fax: 31 53 489 2155

E-mail: d.w.grijpma@tnw.utwente.nl

Mailing Address: University of Twente, Department of Biomaterials Science and Technology, PO Box 217, 7500 AE Enschede, The Netherlands

University of Groningen, University Medical Centre Groningen, Department of Biomedical Engineering, PO Box 196, 9700 AD Groningen, The Netherlands

Collaborative Research Partner Annulus Fibrosus Rupture Program of AO Foundation, Davos, Switzerland

James C. Iatridis,*

Degree: PhD

Telephone: 1 212 241 1517

Fax: 1-212-876-3168

E-mail: james.iatridis@mssm.edu

Mailing Address: Leni & Peter W. May Department of Orthopaedics, Box 1188, Icahn School of Medicine at Mount Sinai, New York, NY, 10029

Collaborative Research Partner Annulus Fibrosus Rupture Program of AO Foundation, Davos, Switzerland

*corresponding author

Abstract:

Herniated intervertebral discs are a common cause of back and neck pain. There is an unmet clinical need to seal annulus fibrosus (AF) defects, since discectomy surgeries address acute pain but are complicated by reherniation and recurrent pain. Copolymers of polyethylene glycol with trimethylene carbonate (TMC) and hexamathylene diisocyanate end-groups were formulated as AF sealants since the hexamathylene diisocyanate form covalent bonds with native AF tissue. TMC adhesives were evaluated and optimized using the design criteria: stable size, strong adherence to AF tissue, high cytocompatibility, restoration of intervertebral disc biomechanics to intact levels following in situ repair, and low extrusion risk. TMC adhesives had high adhesion strength as assessed with a pushout test (150 kPa), and low degradation rates over three weeks in vitro. Both TMC adhesives had shear moduli (220 & 490kPa) similar to, but somewhat higher than AF tissue. The adhesive with three TMC moieties per branch (TMC3) was selected for additional in situ testing because it best matched AF shear properties. TMC3 restored torsional stiffness, torsional hysteresis area and axial range of motion to intact states. However, in a failure test of compressive deformation under fixed 5° flexion, some herniation risk was observed with failure strength of 5.9 MPa compared to 13.5 MPa for intact samples; TMC3 herniated under cyclic organ culture testing. These TMC adhesives performed well during in vitro and in situ testing, but additional optimization to enhance failure strength is required to further this material to advanced screening tests *such as long term degradation*.

Keywords: sealant biomaterial, adhesive, polyethylene glycol (PEG), intervertebral disc herniation, annulus fibrosus repair, intervertebral disc

1. Introduction:

Discectomy is the most effective surgical procedure to treat lower back pain relating to intervertebral disc (IVD) herniation (Asch et al., 2002; Gray et al., 2006; Weinstein et al., 2008). This procedure consists of removing herniated and loose nucleus pulposus (NP) tissue through a small incision in the annulus fibrosus (AF). Defects in the AF due to herniation may be worsened during discectomy procedures and this likely alters IVD biomechanical behaviors and could accelerate IVD degeneration. Incisions in the AF change the biomechanics of the IVD (Elliott et al., 2008; Masuda et al., 2005; Michalek and Iatridis, 2012), especially affecting torque range, disc height and neutral zone characteristics (Iatridis et al., 2013). Discectomy procedures also have a risk of reherniation requiring revision surgery in up to 27% of the patients, depending on the size of the AF defect and the amount of tissue removed (McGirt et al., 2009; Watters and McGirt, 2009).

Currently, there are no widely used and clinically available AF sealants. The development of AF sealants is an active area of research with proposed solutions ranging from hydrogels to mechanical closures devices such as sutures and hardware (Guterl et al., 2013). A full list of injectable AF repair solutions were reviewed (Long et al., 2016), and all have some limitations associated with biological or mechanical incompatibility. Non-injectable AF repair solutions include sutures that do not restore intradiscal pressure (Ahlgren et al., 2000) or that have been discontinued (Bailey et al., 2013), and plugs that have a risk of extrusion (Bron et al., 2010). The Barricaid (Intrinsic Therapeutics, Inc., Woburn, MA) is a shield like structure (Wilke et al., 2013) that allowed retention of NP material and reduced risk of facet degeneration in a clinical trial (Trummer et al., 2013), yet this device adds difficulty to the discectomy procedure, disrupts the endplate, and does not seal the

AF defect. Considering available AF closure solutions, there remains a continued need for an effective and biologically compatible AF adhesive.

An adhesive based on polyethylene glycol (PEG) with trimethylene carbonate (TMC) and hexamathylene diisocyanate (HDI) moieties is a good candidate for AF repair because it is injectable and has material and adhesive properties that are amenable to AF repair. TMC adhesives bond with IVD tissue via nucleophilic attack of amine and hydroxyl groups (Six and Richter, 2000), and form crosslinks via urethane, urea, allophonate and biuret linkages (Pocius, 2012). A formulation with two TMC-HDI moieties per PEG arm (TMC2) had an adhesive strength of 0.35 MPa, as assessed with a lap shear test (Bochyńska et al., 2013). TMC2 had a tensile modulus of 21 MPa (Bochyńska et al., 2013), which is in the range of the linear region of AF tissue (Acaroglu et al., 1995; Green et al., 1993; Guerin and Elliott, 2006; Long et al., 2016; O'Connell et al., 2009). PEG has been approved for therapeutic use alone and as conjugated to protein (FDA Center for Drug Evaluation and Research, 2016), so can be considered biocompatible.

This paper developed and evaluated PEG-TMC adhesives for AF repair. First, we screened two TMC formulations for AF repair and evaluated the effect of increasing the # of TMC-HDI moieties per arm, from 2 to 3 in TMC2 and TMC3 (Figure 1). This part had the following hypotheses: TMC2 and TMC3 have higher adhesion strength than non-adhered AF tissue, low degradation rates and similar shear moduli as native AF tissue. We also hypothesized that cells grown on TMC3 have higher proliferation than those grown on Dermabond. Next, we tested whether TMC3, which performed better during screening tests, could perform well during in situ tests with biomechanics, failure test, and organ culture measurements. We tested the hypotheses that TMC3 would effectively repair IVDs following discectomy in order to

sufficiently restore in situ biomechanics and in situ failure strength to intact IVD levels, and withstand 4 days of cyclic loading without herniation in an organ culture model.

2. Materials and Methods

2.1 Study Design

This study progressed through a testing series of advancing complexity from in vitro screening to in vitro validation and ex vivo analysis (Figure 1). In vitro screening tests evaluated both TMC2 & TMC3 formulations with measurements of adhesion strength using a pushout test, shear modulus using a rheometer, and degradation rate by soaking the adhesive in PBS and measuring dry weight. Based on these results, TMC3 was selected for further screening. In vitro validation included a cytocompatibility test, assessed by growing cells directly on TMC3 and Dermabond and measuring DNA concentration. In situ validations were also applied to TMC3 and included biomechanical tests, failure tests, and organ culture tests to assess cyclic loading.

2.2 Synthesis

TMC adhesives were synthesized in a two-step reaction as described and validated previously (Bochyńska et al., 2013). Briefly, ring-opening polymerization was performed on TMC initiated by PEG with $Sn(Oct)_2$ as a catalyst. The molar ratios, 4:1 and 6:1 for TMC2 and TMC3, resulted in 2 and 3 TMC moieties on each end of the PEG molecule, respectively (Figure 1). Oligomers were added dropwise to a volume of HDI under a flow of nitrogen to ensure an excess of HDI and an inert environment. Excess HDI was removed by precipitation in dry diethyl ether and the PEG400-$(TMC_3\text{-}HDI)_2$ was dried in a vacuum.

The chemicals were purchased from the following vendors: Trimethylene carbonate from ForYou (China), Hexamethylene diisocyanate (HDI) from Merck Schuchardt (Germany), Diethyl ether from Biosolve (the Netherlands), Phosphate buffered saline from B Braun Melsungen AG (Germany), and PEG (M_w = 400 g/mol), acetic anhydride, stannous octoate (tin 2- ethylhexanoate, SnOct2) and chloroform-d (CDCl3) from Sigma Aldrich (Netherlands). PEG was dried at 120° C under vacuum, and diethyl ether was dried over molecular sieves prior to use.

2.3 Adhesion Strength

TMC2 (n = 9) and TMC3 (n = 12) block copolymers were evaluated using a pushout-test described previously (Guterl et al., 2014; Maher et al., 2010). Briefly, PEG-TMC formulations were applied to the center of cylindrical AF specimen (3 mm x ø 8 mm with concentric ø 3mm hole) and cured for 12 hours at 4° C before testing. An indenter (ø 2.8mm) applied displacement at 0.01 mm/s until the adhesive plug underwent a simulated 'herniation'. Adhesion strength was calculated by dividing the failure force by area of contact between adhesive and AF tissue. Failure force was defined by the maximum force before abrupt reduction of force, indicating failure. Adhesion strength for AF press-fit control were obtained from prior tests (Guterl et al., 2014) and is the failure force of passively placed AF tissue.

2.4 Degradation

TMC2 and TMC3, (n = 4 per adhesive per time point) adhesives were prepared and formed into cylindrical plugs by injecting the adhesive into a custom-made Teflon mold (ø 5mm, 1.5 mm thick) (Guterl et al., 2014). Each plug was ~~*weighed initially (Wi) and*~~ soaked in PBS for 1, 7, 14 or 21 days. At each timepoint, glue plugs from

both groups were weighed (Ww), dried in vacuum and weighed again (Wd). Swelling Ratio (Ww/Wd) was calculated from wet weight (Ww) and dry weight (Wd). ~~*Dry Mass Ratio (Wd/Wi) was calculated from initial wet weight (Wi) and dry weight (Wd).*~~

2.5 Shear Modulus

TMC2 and TMC3 (n = 6 per group) adhesives were prepared and formed into cylindrical plugs by injecting the adhesive into a custom-made Teflon mold (3 mm x ø 5 mm). AF tissue plugs were prepared by dissecting AF tissue from frozen bovine caudal IVDs and punched with ø 5 mm biopsy punch. Each gel cured for 4 hours at 37°C submerged in water. Each gel was tested in a parallel plate rheometer (AR2000ex, TA Instruments, New Castle, DE) with a frequency sweep (0.05-10 Hz) at 1% strain under an axial normal force of 2 N (0.1 MPa). Shear modulus is the complex modulus at 1 Hz and 1 % strain.

2.6 Cytocompatibility

Bovine caudal AF cells (n = 3) were seeded in triplicate in each condition in 48-well plates at 24,000 cells/well; the wells were either coated with TMC3 or Dermabond, or left uncoated (No Adhesive; i.e. tissue culture plastic: polystyrene). *TMC3 was selected for further screening since TMC3 and TMC2 had similar adhesion strengths and degradation profiles, and TMC3 had similar shear modulus to AF tissue*. Cells were cultured for 1, 3 or 7 days at 37° C, 5% CO_2 and ambient oxygen. Cells were grown in high glucose Dulbecco's Modified Eagle Medium (DMEM), supplemented with 10% Fetal Bovine Serum (FBS), 1% Pen/Strep, and 0.2% ascorbic acid. Cells were then lysed and the double-stranded DNA content was quantified using fluorescent dye (QuantiFluor® dsDNA System, Promega, Madison, WI) and a

microplate reader (SpectraMax M5, Molecular Devices, Sunnyvale, CA). Dermabond and cell culture plate plastic (tissue culture polystyrene) were used as limiting case controls. Dermabond has known cytotoxicity, and is used as a control here since it is a strong adhesive and it has also been tested in vivo in the disc (Kang et al., 2015). Conversely, cell culture plastic is the control for the limiting case of fastest cell growth expected for these cells.

2.7 Biomechanics

Six skeletally mature bovine tails were obtained from a local abattoir (Green Village Packing, Green Village, NJ) and twelve motion segments (vertebra-IVD-vertebra) were dissected from two caudal levels (cc 2-3 & cc 3-4). Each motion segment per tail was distributed to one of two groups (n = 6 *per group): Sham ~~Injured (Control)~~ or TMC3 (repaired)*. Bovine coccygeal IVDs were chosen because the size is comparable to human lumbar IVD (Illien-Jünger et al., 2013). After dissection, motion segments were wrapped in saline soaked tissue and frozen until testing. The night before testing, samples were thawed overnight in Phosphate Buffered Saline (Fisher BioReagents, Fischer Scientific, Pittsburgh, PA), and potted in polymethylmethacrylate (Henry Schein Inc., Melville, NY).

All motion segments were evaluated in a repeated measures test that included 3 tests: Intact, ~~*and*~~ Discectomy, and ~~*finally*~~ in the Experimental condition: either *TMC3 (repaired) or Sham (not repaired)* ~~*with (TMC3) or without repair (Sham)*~~ (Figure 2). The *first test, in the Intact condition,* occurred after overnight swelling equilibration in PBS. *The second test, in the Discectomy condition, occurred after overnight swelling equilibration in PBS and discectomy.* ~~*After the first test, all IVDs were soaked overnight in PBS and then subjected to discectomy.*~~ The discectomy consisted of a 5

mm biopsy punch defect through the posterolateral AF and removal of approximately 25 % of the NP (145 ± 17 mg). The third test, *in the Experimental condition, occurred* ~~*mechanical test after discectomy was performed for all IVDs before undergoing*~~ after group specific treatment (Figure 2). The TMC3 group was repaired with TMC3 by retrograde injection, left at ~~*then cured at*~~ room temperature for thirty minutes *to cure*, submerged in PBS overnight and subjected to the final mechanical test. The Sham group was submerged in PBS *overnight and subjected to the final mechanical test* ~~*tested.*~~

The mechanical test consisted of *multistep cyclic loading in axial compression, tension and torsion. First, there was a one minute ramp to -50 N preload and a ten minute hold at this load.* ~~*a one- minute ramp to 50 N in compression, a ten minute 50 N axial preload,*~~ The preload was followed by 20 cycles of axial loading to forces equivalent *0.25 MPa (tension) and 0.50 MPa (compression)* nominal axial stresses *at* 0.1 Hz. The axial loading was followed by 20 torsion cycles from ± 4° at 0.1 Hz (Figure 2). The displacement of the torsion cycles ~~*was ± 4°, which*~~ is approximately the maximum physiological rotational range of motion of human lumbar motion segments (Li et al., 2009; Pearcy and Tibrewal, 1984; Xia et al., 2010). Specimens were tested with an MTS Servohydraulic system (Bionix 858, MTS, Eden Prairie, MN, USA).

Herniation was monitored with a video camera throughout the loading procedures. Force, displacement, torque and rotation were recorded at 100 Hz. The biomechanical variables were calculated using the second to last cycle using a custom MATlab code (Mathworks, Natick, MA, USA). The compressive, tensile and torsional stiffness were calculated as the top 20% of the axial load or rotation of the force-displacement or torque-rotation curves. The axial range of motion (ROM) and

torque range were calculated as the total displacement or torque developed. All parameters except hysteresis area were normalized by dividing by the corresponding value from the first (Intact) test. The hysteresis area was calculated as the area between the loading and unloading force-displacement or torque-rotation curves. The neutral zone stiffness was calculated as the slope of 10 data points (0.1 sec) in the center of the force-displacement of torque-rotation curves.

2.8 Failure Strength

Vertebra-IVD-vertebra segments from nine tails (levels cc2-3, cc3-4 and cc4-5) were dissected as previously described except that the vertebral bodies were sectioned approximately 4-5mm above endplates with a diamond blade saw (IsoMet 1000 Precison Cutter, Buehler, Lake Bluff, IL). The motion segments were distributed to either Intact, Discectomy or TMC3 groups (n=9 *per group*). Intact samples underwent no treatment. The Discectomy and TMC3 samples underwent a posterolateral 4 mm biopsy punch defect and removal of 150-170 mg of nuclear and annular material using a rongeur. The TMC3 samples were repaired as described above. All samples were soaked in PBS overnight before testing. The diameter and disc height of each sample was measured three times at different locations and averaged. Each sample was subjected to *monotonically* increasing compressive axial displacement (2 mm/min) under a fixed 5° bending with the posterolateral injured or repaired face at the outside of the bend (i.e. the defect face had a larger disc height than the opposite side) as described previously (Vergroesen, Kingma, et al., 2015). Force and subsidence were measured through the test and extrusion was monitored by video. Failure strength and subsidence until failure were identified by inspecting the force trace and corresponding video to determine the point at which NP tissue breached

the boundary of the IVD. Extrusion of the TMC3 glue was also monitored. The mechanism of failure was identified as follows: Endplate failure occurred with a single maximum force in a monotonically increasing force trace. Nucleus herniation failure occurred with incremental micro-failures and a subsequent increase in the force trace.

2.9 Organ Culture

Bovine IVDs with endplates were randomly distributed among 3 groups: Intact, Discectomy and TMC3 repair (n=3 *per group*) and prepared as described previously (Gantenbein et al., 2006; Illien-Jünger et al., 2010; Walter, Illien-Jünger, et al., 2014). For Discectomy and TMC3 IVDs, the discectomy was initiated on the posterolateral side of the IVD with a 4 mm biopsy punch to the center of the IVD, followed by tissue removal with a rongeur. IVDs were then cultured for 4 days with applied loading that *simulated the diurnal cycle and two bouts of rigorous loading starting on Day 2.* Loading consisted of diurnal loading (8 h: 0.2 MPa/16 h: 0.3 MPa) with 2 five-hour bouts of 'exercise' (0.3±0.2 MPa @ 0.1 Hz) during the daytime cycle, similar to that described(Walter, Illien-Jünger, et al., 2014). Over the 4 day culture period, *10,800 cycles of loading were applied.* Immediately after culture, discs were fixed in zinc formalin (Z-Fix®, Anatech LTD, Battle Creek MI) for at least 48 hours, embedded in methyl-methacrylate (MMA) and sectioned as previously described (Laudier et al., 2007; Walter, Torre, et al., 2014). Sections were then stained with Picrosirius Red/Alcian Blue (Gruber et al., 2009) and imaged with an upright light microscope (AxioImager Z1, Ziess).

2.10 Statistics

A one-way non-parametric ANOVA (Friedman's) with correction for multiple comparisons (Dunn's) was used to assess differences between treatments for adhesion, shear modulus, failure strength and subsidence. A one-way non-parametric ANOVA with multiple comparisons test was also used to test differences between means of the Intact condition, Discectomy condition and the final condition (either TMC3 or Sham) for biomechanics. A two way non-parametric ANOVA with correction for multiple comparisons was used to detect differences between treatments and timepoints for cytocompatibility and degradation. Significance was assessed at $\alpha=0.05$ level. All statistics were calculated with Prism version 6.04 for Windows (GraphPad Software, La Jolla California USA). All data is presented mean ± standard deviation and all error bars are standard deviation.

3. Results

3.1 Adhesion Strength

For the pushout test, TMC2 and TMC3 had significantly higher adhesion strength than the AF pressfit control (Figure 3).

3.2 Degradation

The *swelling ~~dry mass~~* ratio (Ww/Wd)*, wet weight over dry weight, ~~amount of dry mass present at each time point normalized by the initial mass,~~* remained unchanged for TMC3 and TMC2 through 3 weeks *~~and for TMC2 for the last week. A small but statistically significant decrease of dry mass ratio was observed for TMC2 for the first two weeks~~ (*Figure 3).

3.3 Shear Modulus

The shear modulus of TMC2 was greater than AF tissue (Figure 3). Since the shear modulus of TMC3 was not significantly greater than AF tissue, TMC3 was prioritized for further analysis ~~*(Figure 3).*~~

3.4 Cytocompatibility

DNA concentration significantly increased from Day 1 to 7 for the Plastic (i.e. no adhesive) group, while no changes in DNA content was observed for Dermabond or TMC3 treated cells. DNA concentration was higher for cells grown on plastic (3759.8 ± 2797.0 ng/mL) compared to Dermabond (17.1 ± 6.6 ng/mL) and TMC3 (1026.3 ± 955.3 ng/mL) at Day 7 ($p < 0.05$), and DNA concentration trended higher for cells grown on TMC3 compared to Dermabond ($p = 0.09$) (Figure 4).

3.5 Biomechanics

Discectomy resulted in increased axial ROM, decreased torsion hysteresis area, torsion stiffness, and torque range (Figure 5) compared to the intact condition for both groups: Sham and TMC3 repaired. This change was present in the third test for the Sham group for only axial ROM, torsion hysteresis area and torsional stiffness, indicating the effect of the injury on these parameters was constant through the two days and both tests for the Sham group. Of these parameters, the TMC3 group had similar values to those of the Intact condition for axial ROM, torsion hysteresis area and torsional stiffness, indicating restoration to intact values. There was no change between Intact and Discectomy conditions for axial hysteresis, compressive stiffness and tensile stiffness (not shown).

None of the six successfully repaired specimens herniated.

3.6 Failure Strength

The Injured and TMC3 repaired samples had lower failure strengths (4.5 ± 2.7 MPa and 5.9 ± 4.2 MPa, respectively) and lower subsidence to failure (2.09 ± 0.67 and 2.29 ± 0.69 mm, respectively), defined by the extrusion of NP material, than did the intact samples (13.5 ± 4.2 MPa and 3.30 ± 0.54 mm) (Figure 6). TMC3 repair extruded at lower nominal axial stress (force/area) and subsidence than the extrusion of nuclear tissue (0.80 ± 0.63 MPa and 0.945 ± 0.402 mm, respectively). In both, the injured and TMC3 groups, 9/9 samples failed by herniation compared to 1/9 in the intact group, in which the mechanism of failure was endplate fracture.

3.7 Organ Culture

In organ culture, 2 of 3 TMC3 repairs herniated after 4 days of culture. In Picrosirius red/Alcian blue stained histological sections, the TMC3 repaired group had a rectangular shaped defect where the TMC3 adhesive was injected whereas the discectomy group had a triangular shaped defect due to NP swelling and additional tissue deformations. Upon high magnification inspection, there was evidence that the TMC3 plug dislodged some AF tissue upon herniation (Figure 7B) and the discectomy sample had herniated NP material. At the AF defect surface, the TMC3 repaired sample had less disrupted AF structure than the discectomy group which had a more disorganized AF structure at the defect edge (Figure 7).

4. Discussion

TMC2 and TMC3 PEG-TMC compositions were evaluated to assess their capacity to serve as AF adhesives following discectomy. TMC2 and TMC3 had similarly high adhesion strengths and low degradation rates but TMC2 had a shear modulus substantially higher than native AF tissue. Since TMC2 had a material property mismatch, TMC3 was prioritized for further in vitro and in situ validation tests with assessments of cytocompatibility, in situ biomechanics, in situ failure and organ culture. TMC3 allowed cell proliferation, suggesting good cytocompatibility, partially restored motion segment biomechanics to intact levels, and was easy to inject into the IVD. However, TMC3 had a high risk of herniation during the in situ failure test and cyclic organ culture. Further optimization is therefore required and may consist of chemical modifications to change the TMC material properties to be more similar to the AF, and increasing adhesion strength by reducing hydrophobicity and increasing wetting behaviors.

TMC2 and TMC3 had high adhesion strengths (150 kPa) as measured by pushout testing, likely due to the formation of covalent bonds with the native IVD tissue. Comparing with other proposed AF sealants proposed in the literature, TMC2 and TMC3 both had higher adhesive strength than fibrin (72.2 ± 29 kPa), fibrin crosslinked with genipin (67.5 ± 31 kPa) (Guterl et al., 2014), Poly(*N*-isopropylacrylamide–poly(ethylene glycol)/ poly(ethylene imine) with gluteraldehyde crosslinker (1.4-2.5 kPa) (Vernengo et al., 2010), Poly(*N*-isopropylacrylamide) + chondroitin sulfate ± aldehyde modified chondroitin sulfate (1.1 kPa-1.8 kPa) (Wiltsey et al., 2015), and aligned nanofibrous poly-ε-caprolactone scaffold (55-125

kPa) (Nerurkar et al., 2009), but not Dermabond (700 kPa) (Bochyńska et al., 2016). The electrophilic isocyanate groups are vulnerable to nucleophilic attack from amine and hydroxyl groups in intervertebral disc tissue, yielding urethanes and ureas. Amine and hydroxyl groups are found in sulfated glucosaminoglycans present in the IVD (Melrose and Roughley, 2014). The urea and urethane groups can further react with excess isocynate to form allophonate and biuret linkages, also resulting in crosslinkages and adherence (Pocius, 2012). Both TMC2 and TMC3 were stable through time and were not prone to hydrolytic cleavage in phosphate buffered saline after 3 weeks, as compared with fibrin which is known to degrade rapidly(Guterl et al., 2014).

Cyanoacrylates have toxic byproducts resulting in seroma formation, tissue necrosis and chronic foreign body giant cell reaction when placed beneath the skin (Mobley et al., 2002), and shorter polymers degrade faster, resulting in higher toxicity. Dermabond therefore has a reduced cytocompatibility, which presumably allowed it to be approved only for topical use in the United States (Administration, 1998; Medhekar and Melkerson, 2010). We hypothesized that TMC3 would have increased cytocompatibility compared to Dermabond (2-Octyl cyanoacrylate, M_w = 209.20 g/mol) since PEG-TMC adhesives have higher molecular weights (TMC2 $M_w \cong$ 1,038 g/mol, TMC3 $M_w \cong$ 1,186 g/mol) (Figure 1) and form large interbranching networks, thus degrading more slowly and enabling transport and release of potential cytotoxic degradation products. Additionally, PEG-based adhesives such as Duraseal and Coseal are currently in clinical use (Mehdizadeh and Yang, 2012). We found that cells grew substantially more rapidly on TMC3 than on Dermabond. However, decreased cytocompatibility for both groups was identified since we found that at day

7, Dermabond and TMC3 had lower DNA concentrations than cells grown on plastic. The toxicity of Dermabond is likely due to cyanoacrylate degradation into cyanoacetate and formaldahyde via the inverse Knoevenagel reaction, but could be due to other metabolic pathways (Hubbard et al., 2014). The reduction of DNA content of cells grown on TMC3 may be due to the buildup of carbonic acid resulting from the release of carbon dioxide after reaction with water (Six and Richter, 2000), or may be due to decreased adhesion. Since the DNA concentration of cells grown onTMC3 was similar to that of cells grown on plastic and trended to be higher than those on Dermabond, we considered this acceptable.

Discectomy resulted in significantly increased axial ROM, and significantly reduced torsion hysteresis, torsion stiffness and torque range. These results are consistent with previous findings that torsion mechanics are sensitive to AF injury, including loss of stiffness and increased range of motion (Iatridis et al., 2013). Defects larger than 40% of the disc height are known to induce repeatable and measurable effects (Elliott et al., 2008) and we used a 5 mm injury (~50% disc height) for biomechanics to induce large effects. TMC3 resulted in recovery of torsional stiffness, hysteresis, and axial ROM to the intact condition, but not in torque range. This restoration of three biomechanical parameters shows promise.

Failure testing and organ culture testing demonstrated a risk of herniation. Specifically, failure strength was similar for TMC3 and discectomy groups, and some herniation of TMC3 was observed during the physiological cyclic loading in organ culture testing. The failure strength of intact (13.5 ± 4.2 MPa) and injured bovine IVDs (4.5 ± 2.7 MPa) was similar to the failure strength of intact (12.5 ± 4.4 MPa) and injured (punctured with 2.4 mm hypodermic needle; 6.5 ± 3.6 MPa) lumbar IVDs

from skeletally mature Dutch milk goats (Vergroesen, Bochyńska, et al., 2015). A 4 mm diameter defect was used in our failure strength and organ culture studies as a large repeatable defect approximately 40% of the disc height. The failure strength of TMC3 (5.9 ± 4.2 MPa) was similar to that of TMC1 (9.8 ± 6.1 MPa) (Vergroesen, Bochyńska, et al., 2015). Interestingly, TMC3 failed at lower stresses than TMC1, and we believe it is likely that TMC3 did not wet the surface of the AF since it has greater hydrophobicity. Water content in both TMC2 and TMC3 was low, indicating some hydrophobicity from the TMC groups, possibly influencing the interaction with the AF, which is about 75% water (Antoniou et al., 1996). However, it is possible that the shear modulus of TMC3 was too high and this AF-TMC3 material mismatch resulted in stress concentrations that were responsible for the herniation risk. Consequently, new formulations of TMC may must be developed that can result in better wetting characteristics, perhaps by increasing the hydrophilic PEG to hydrophobic TMC ratio while also providing biochemical modifications allowing better matching to native AF tissue material properties.

TMC3 herniated in 2 out of 3 samples during organ culture experiments. A useful future direction elucidated by this work is the importance of applying a physiologically relevant failure test early in the screening process to assess in vivo extrusion risk. Adhesion strength and failure strength test used loading rates that have been published to allow better comparison with the literature, but herniations are expected to occur at higher rates and results may be results may be rate dependent. Extrusion is a risk that has sidelined many annular repair strategies (Bron et al., 2010), and is important to address this risk early in the development for annular repair strategies. *Another important parameter to assess in future tests is long term degradation and*

cytocompatibility since the effect of degradation byproducts of these adhesives is unknown and may impact in vivo performance.

5. Conclusions

PEG-TMC based adhesives were screened and validated as AF sealants using a robust testing paradigm. TMC3 exhibited high adhesive strength, slow degradation, high cytocompatibility, and good in situ biomechanical performance but extruded at high stresses and under cyclic loading. Further optimization of TMC is necessary to promote better tissue integration and prevent herniation, possibly with formulations that increase wetting behaviors and allow better matching of AF compressive and shear material properties.

Acknowledgements:

NIH grants R01AR057397 & T32 GM062754; Whitaker Foundation International Fellow Program and the Collaborative Research Program of the AO Foundation.

The authors gratefully acknowledge the development of this adhesive by Agnieszka I. Bochyńska and technical contribution and helpful discussions from Philip Nasser.

Author Disclosure Statement:

Long, RG. No competing financial disclosures exist.

Hom, WW. No competing financial interests exist.

Rotman, SG. No competing financial interests exist.

Grijpma, DW. No competing financial interests exist.

Assael, DJ. No competing financial interests exist.

Illien-Junger S. No competing financial interests exist.

Iatridis, JC. No competing financial interests exist.

Name and Address of the reprint author:

James C. Iatridis, PhD

E-mail: james.iatridis@mssm.edu

Mailing Address: Leni & Peter W. May Department of Orthopaedics, Icahn School of Medicine at Mount Sinai, New York, NY, 10029

6. References

Acaroglu, E.R., Iatridis, J.C., Setton, L.A., Foster, R.J., Mow, V.C., Weidenbaum, M., 1995. Degeneration and aging affect the tensile behavior of human lumbar anulus fibrosus. Spine 20, 2690–2701.

Administration, F.A.D., 1998. Summary of safety and effectiveness data: Dermabond 1–17.

Ahlgren, B.D., Lui, W., Herkowitz, H.N., Panjabi, M.M., Guiboux, J.P., 2000. Effect of anular repair on the healing strength of the intervertebral disc: a sheep model. Spine 25, 2165–2170.

Antoniou, J., Steffen, T., Nelson, F., Winterbottom, N., Hollander, A.P., Poole, R.A., Aebi, M., Alini, M., 1996. The human lumbar intervertebral disc: evidence for changes in the biosynthesis and denaturation of the extracellular matrix with growth, maturation, ageing, and degeneration. J. Clin. Invest. 98, 996–1003.

Asch, H.L., Lewis, P.J., Moreland, D.B., Egnatchik, J.G., Yu, Y.J., Clabeaux, D.E., Hyland, A.H., 2002. Prospective multiple outcomes study of outpatient lumbar microdiscectomy: should 75 to 80% success rates be the norm? J Neurosurg 96, 34–44.

Bailey, A., Araghi, A., Blumenthal, S., Huffmon, G.V., 2013. Prospective, Multicenter, Randomized, Controlled Study of Anular Repair in Lumbar Discectomy. Spine 38, 1161–1169.

Bochyńska, A.I., Sharifi, S., van Tienen, T.G., Buma, P., Grijpma, D.W., 2013. Development of Tissue Adhesives Based on Amphiphilic Isocyanate-Terminated Trimethylene Carbonate Block Copolymers. Macromol. Symp. 334, 40–48.

Bochyńska, A.I., Van Tienen, T.G., Hannink, G., Buma, P., Grijpma, D.W., 2016. Development of biodegradable hyper-branched tissue adhesives for the repair of meniscus tears. Acta Biomaterialia 32, 1–9.

Bron, J.L., van der Veen, A.J., Helder, M.N., van Royen, B.J., Smit, T.H., 2010. Biomechanical and in vivo evaluation of experimental closure devices of the annulus fibrosus designed for a goat nucleus replacement model. Eur Spine J 19, 1347–1355.

Elliott, D.M., Yerramalli, C.S., Beckstein, J.C., Boxberger, J.I., Johannessen, W., Vresilovic, E.J., 2008. The effect of relative needle diameter in puncture and sham injection animal models of degeneration. Spine 33, 588–596.

FDA Center for Drug Evaluation and Research (Ed.), 2016. Drugs@FDA. Office of Communications

Division of Online Communications. URL http://www.accessdata.fda.gov/scripts/cder/drugsatfda/index.cfm?fuseaction=Search.SearchAction&SearchTerm=PEG&SearchType=BasicSearch&#totable

Gantenbein, B., Grünhagen, T., Lee, C.R., van Donkelaar, C.C., Alini, M., Ito, K., 2006. An in vitro organ culturing system for intervertebral disc explants with vertebral endplates: a feasibility study with ovine caudal discs. Spine 31, 2665–2673.

Gray, D.T., Deyo, R.A., Kreuter, W., Mirza, S.K., Heagerty, P.J., Comstock, B.A., Chan, L., 2006. Population-based trends in volumes and rates of ambulatory lumbar spine surgery. Spine 31, 1957–63– discussion 1964.

Green, T.P., Adams, M.A., Dolan, P., 1993. Tensile properties of the annulus fibrosus II. Ultimate tensile strength and fatigue life. Eur Spine J 2, 209–214.

Gruber, H.E., Ingram, J., Jr, E.N.H., 2009. An improved staining method for intervertebral disc tissue. Biotechnic & Histochemistry 77, 81–83.

Guerin, H.A.L., Elliott, D.M., 2006. Degeneration affects the fiber reorientation of human annulus fibrosus under tensile load. J Biomech 39, 1410–1418.

Guterl, C.C., See, E.Y., Blanquer, S.B.G., Pandit, A., Ferguson, S.J., Benneker, L.M., Grijpma, D.W., Sakai, D., Eglin, D., Alini, M., Iatridis, J.C., Grad, S., 2013. Challenges and strategies in the repair of ruptured annulus fibrosus. Eur Cell Mater 25, 1–21.

Guterl, C.C., Torre, O.M., Purmessur, D., Khyati, D., Likhitpanichkul, M., Hecht, A.C., Nicoll, S.B., Iatridis, J.C., 2014. Characterization of Mechanics and Cytocompatibility of Fibrin-Genipin Annulus Fibrosus Sealant with the Addition of Cell Adhesion Molecules. Tissue Eng Part A 20, 140506130038007.

Hubbard, D., Brayden, D.J., Ghandehari, H., 2014. Nanopreparations for Oral Administration, in: Torchilin, V. (Ed.), Handbook of Nanobiomedical Research: Fundamentals, Applications and Recent Developments. World Scientific, pp. 153–204.

Iatridis, J.C., Nicoll, S.B., Michalek, A.J., Walter, B.A., Gupta, M.S., 2013. Role of biomechanics in intervertebral disc degeneration and regenerative therapies: what needs repairing in the disc and what are promising biomaterials for its repair? The Spine Journal 13, 243–262.

Illien-Jünger, S., Gantenbein-Ritter, B., Grad, S., Lezuo, P., Ferguson, S.J., Alini, M., Ito, K., 2010. The combined effects of limited nutrition and high-frequency loading on intervertebral discs with endplates. Spine 35, 1744–1752.

Illien-Jünger, S., Walter, B.A., Mayer, J.E., Hecht, A.C., Iatridis, J.C., 2013. Intervertebral Disc Culture Models and Their Applications to Study Pathogenesis and Repair, in: Shapiro, I.M., Risbud, M.V. (Eds.), The Intervertebral Disc. Springer Vienna, Vienna, pp. 353–371.

Kang, R., Li, H., Lysdahl, H., Quang Svend Le, D., Chen, M., Xie, L., Bünger, C., 2015. Cyanoacrylate medical glue application in intervertebral disc annulus defect repair: Mechanical and biocompatible evaluation. J. Biomed. Mater. Res n/a–n/a.

Laudier, D.M., Schaffler, M.B., Flatow, E.L., Wang, V.M., 2007. Novel procedure for high-fidelity tendon histology. Journal of Orthopaedic Research 25, 390–395.

Li, G., Wang, S., Passias, P., Xia, Q., Li, G., Wood, K., 2009. Segmental in vivo vertebral motion during functional human lumbar spine activities. Eur Spine J 18, 1013–1021.

Long, R.G., Torre, O.M., Hom, W.W., Assael, D.J., Iatridis, J.C., 2016. Design Requirements for Annulus Fibrosus Repair: Review of Forces, Displacements, and Material Properties of the Intervertebral Disk and a Summary of Candidate Hydrogels for Repair. J Biomech Eng 138, 021007.

Maher, S.A., Mauck, R.L., Rackwitz, R.A., Tuan, R.S., 2010. A Nano-Fibrous Cell Seeded Hydrogel Promotes Integration in a Cartilage Gap Model. Journal of Anatomy 4, 25.

Masuda, K., Aota, Y., Muehleman, C., Imai, Y., Okuma, M., Thonar, E.J., Andersson, G.B., An, H.S., 2005. A novel rabbit model of mild, reproducible disc degeneration by an anulus needle puncture: correlation between the degree of disc injury and radiological and histological appearances of disc degeneration. Spine 30, 5–14.

McGirt, M.J., Eustacchio, S., Varga, P., Vilendecic, M., Trummer, M., Gorensek, M., Ledic, D., Carragee, E.J., 2009. A prospective cohort study of close interval computed tomography and magnetic resonance imaging after primary lumbar discectomy: factors associated with recurrent disc herniation and disc height loss. Spine 34, 2044–2051.

Medhekar, N., Melkerson, M.N., 2010. Section 510(k) premarket notification 1–6.

Mehdizadeh, M., Yang, J., 2012. Design Strategies and Applications of Tissue Bioadhesives. Macromol. Biosci. 13, 271–288.

Melrose, J., Roughley, P., 2014. Proteoglycans of the Intervertebral Disc, in: Shapiro, I.M., Risbud, M.V. (Eds.), The Intervertebral Disc. Springer Vienna, Vienna, pp. 53–77.

Michalek, A.J., Iatridis, J.C., 2012. Height and torsional stiffness are most sensitive to annular injury in large animal intervertebral discs. The Spine Journal 12, 425–432.

Mobley, S.R., Hilinski, J., Toriumi, D.M., 2002. Surgical tissue adhesives. Facial Plast Surg Clin North Am 10, 147–154.

Nerurkar, N.L., Baker, B.M., Sen, S., Wible, E.E., Elliott, D.M., Mauck, R.L., 2009. Nanofibrous biologic laminates replicate the form and function of the annulus fibrosus. Nat Mater 8, 986–992.

O'Connell, G.D., Guerin, H.L., Elliott, D.M., 2009. Theoretical and Uniaxial Experimental Evaluation of Human Annulus Fibrosus Degeneration. J Biomech Eng 131, 111007.

Pearcy, M.J., Tibrewal, S.B., 1984. Axial rotation and lateral bending in the normal lumbar spine measured by three-dimensional radiography. Spine 9, 582–587.

Pocius, A.V., 2012. Adhesion and Adhesives Technology, Third Edition. ed, Adhesion and Adhesives Technology: An Introduction. Carl Hanser Verlag GmbH & Co. KG.

Six, C., Richter, F., 2000. Isocyanates, Organic. Ullman's Encyclopedia of Industrial Chemsitry, Weinheim, Germany.

Trummer, M., Eustacchio, S., Barth, M., Klassen, P.D., Stein, S., 2013. Protecting facet joints post-lumbar discectomy: Barricaid annular closure device reduces risk of facet degeneration. Clin Neurol Neurosurg 115, 1440–1445.

Vergroesen, P.-P.A., Bochyńska, A.I., Emanuel, K.S., Sharifi, S., Kingma, I., Grijpma, D.W., Smit, T.H., 2015. A Biodegradable Glue for Annulus Closure. Spine 40, 622–628.

Vergroesen, P.P.A., Kingma, I., Emanuel, K.S., Hoogendoorn, R.J.W., Welting, T.J., van Royen, B.J., van Dieën, J.H., Smit, T.H., 2015. Mechanics and biology in intervertebral disc degeneration: a vicious circle. Osteoarthritis and Cartilage.

Vernengo, J., Fussell, G.W., Smith, N.G., Lowman, A.M., 2010. Synthesis and characterization of injectable bioadhesive hydrogels for nucleus pulposus replacement and repair of the damaged intervertebral disc. J. Biomed. Mater. Res 93B, 309–317.

Walter, B.A., Illien-Jünger, S., Nasser, P.R., Hecht, A.C., Iatridis, J.C., 2014. Development and validation of a bioreactor system for dynamic loading and mechanical characterization of whole human intervertebral discs in organ culture. J Biomech 47, 2095–2101.

Walter, B.A., Torre, O.M., Laudier, D.M., Naidich, T.P., Hecht, A.C., Iatridis, J.C., 2014. Form and function of the intervertebral disc in health and disease: a morphological and stain comparison study. Journal of Anatomy n/a–n/a.

Watters, W.C., McGirt, M.J., 2009. An evidence-based review of the literature on the consequences of conservative versus aggressive discectomy for the treatment of primary disc herniation with radiculopathy. The Spine Journal 9, 240–257.

Weinstein, J.N., Lurie, J.D., Tosteson, T.D., Tosteson, A.N.A., Blood, E.A., Abdu, W.A., Herkowitz, H., Hilibrand, A., Albert, T., Fischgrund, J., 2008. Surgical versus nonoperative treatment for lumbar disc herniation: four-year results for the Spine Patient Outcomes Research Trial (SPORT). Spine 33, 2789–2800.

Wilke, H.-J., Ressel, L., Heuer, F., Graf, N., Rath, S., 2013. Can prevention of a reherniation be investigated? Establishment of a herniation model and experiments with an anular closure device. Spine 38, E587–E593.

Wiltsey, C., Christiani, T., Williams, J., Scaramazza, J., Van Sciver, C., Toomer, K., Sheehan, J., Branda, A., Nitzl, A., England, E., Kadlowec, J., Iftode, C., Vernengo, J., 2015. Thermogelling bioadhesive scaffolds for intervertebral disk tissue engineering: Preliminary in vitro comparison of aldehyde-based versus alginate microparticle-mediated adhesion. Acta Biomaterialia 16, 71–80.

Xia, Q., Wang, S., Kozanek, M., Passias, P., Wood, K., Li, G., 2010. In-vivo motion characteristics of lumbar vertebrae in sagittal and transverse planes. J Biomech 43, 1905–1909.

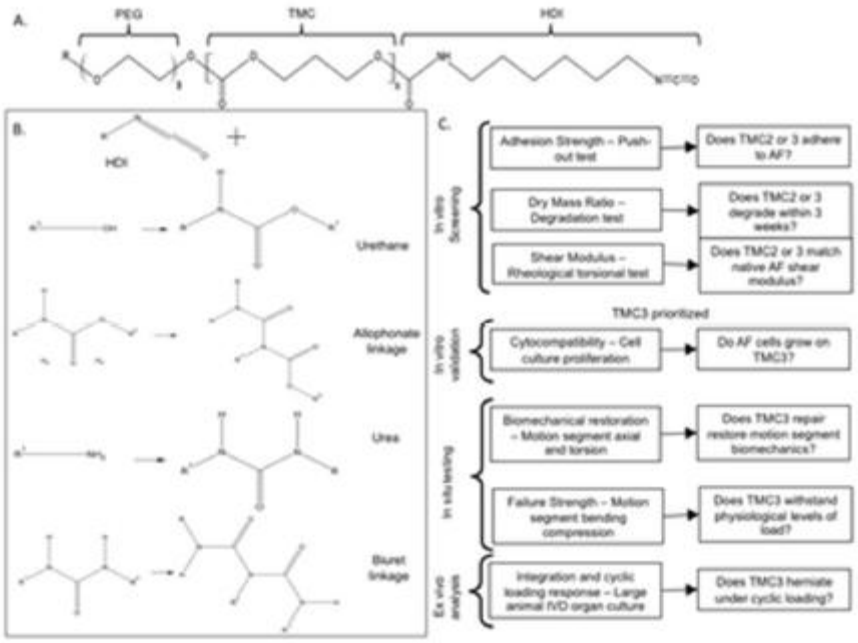

Figure 1. PEG with HDI reactions with native tissue proteins; study design progresses from screening to validation. (A) TMC2 and TMC3 are block copolymers of PEG and HDI with n = 2 and 3 and molecular weights of about 1,038 g/mol and 1,186 g/mol, respectively. (B) The isocyanate groups in the HDI end groups form urethane, urea, allophonate and biuret linkages when reacted with alcohols and amines in IVD tissue. Reactions from Pocius, 2012. (C) The study design progresses from simpler screening tests to increasingly complex tests including in vitro, in situ and ex vivo validation.

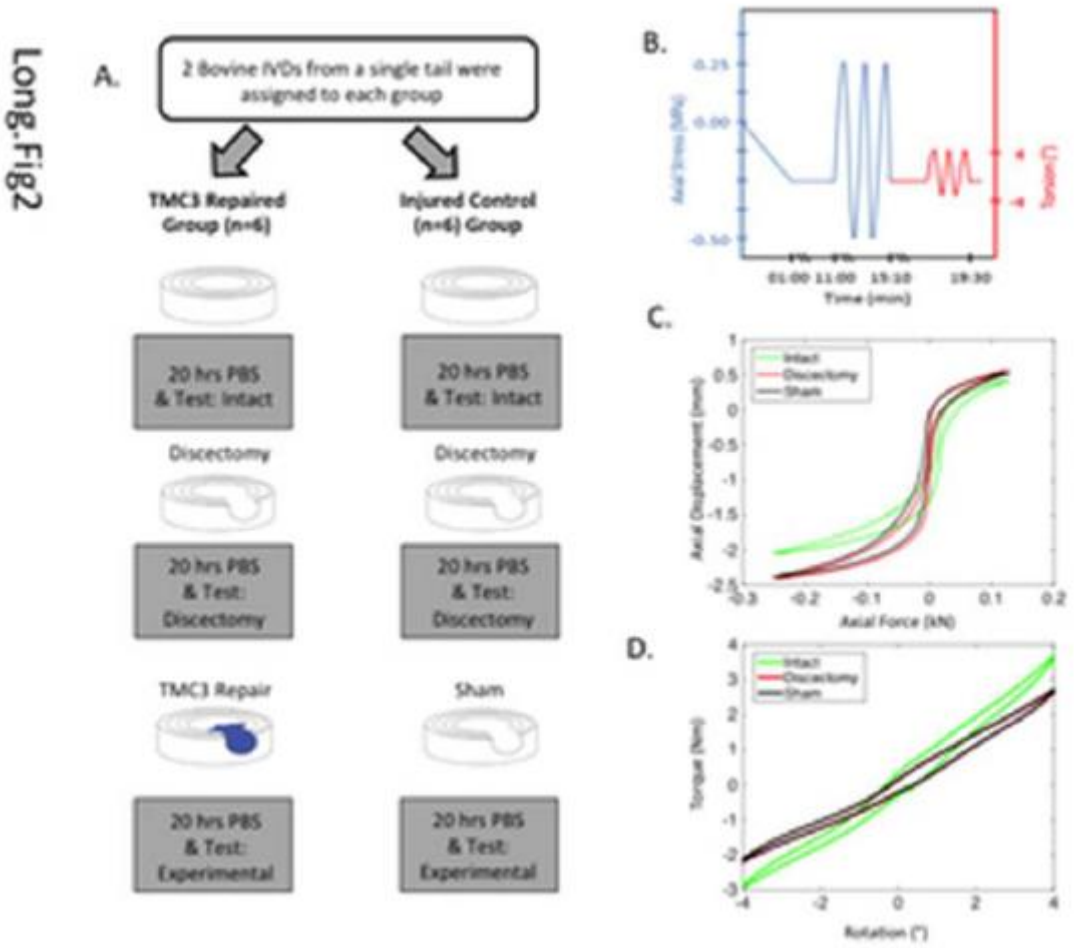

Figure 2. In situ biomechanics testing study design and sample results. (A) Each specimen was tested under axial force and torsion conditions three times as a repeated measured test: Intact, Discectomy and Experimental. The experimental condition involved TMC3 repair (TMC3) or non-treated injured control (Sham). (B) The loading protocol consisted of a 1 minute ramp, 10 minute compression, 20 cycles of tension and compression (0.25 to -0.50 MPa) and 20 cycles of torsion (± 4°). The 2nd to last (C) force-displacement and (D) torque-rotation traces were analyzed; the representative discectomy trace (red) was different than the intact (green).

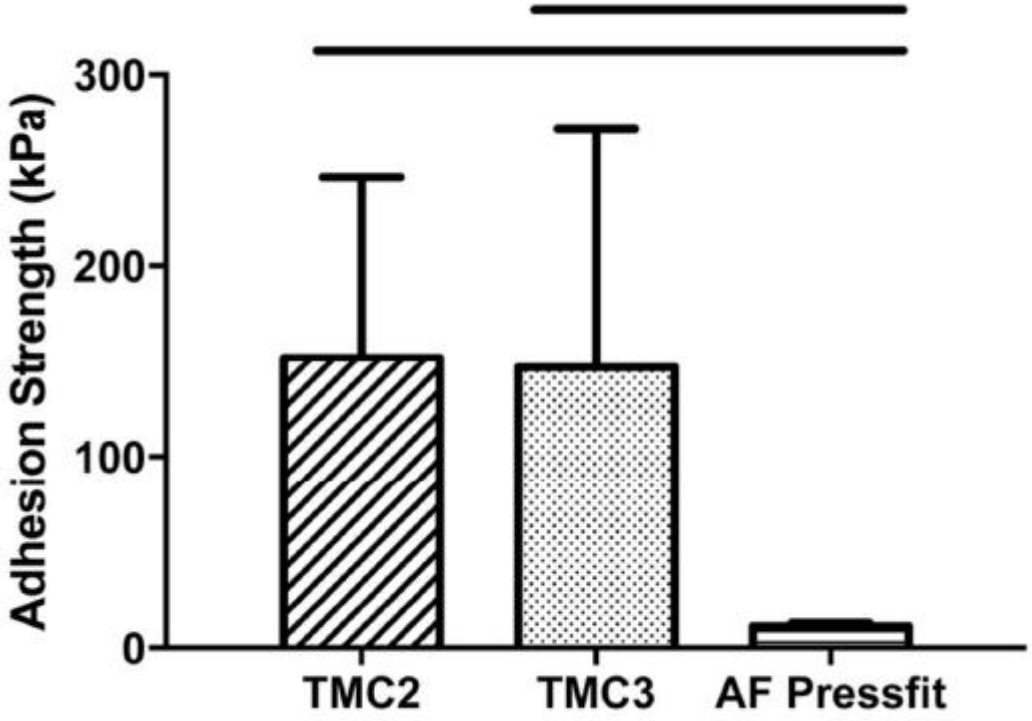

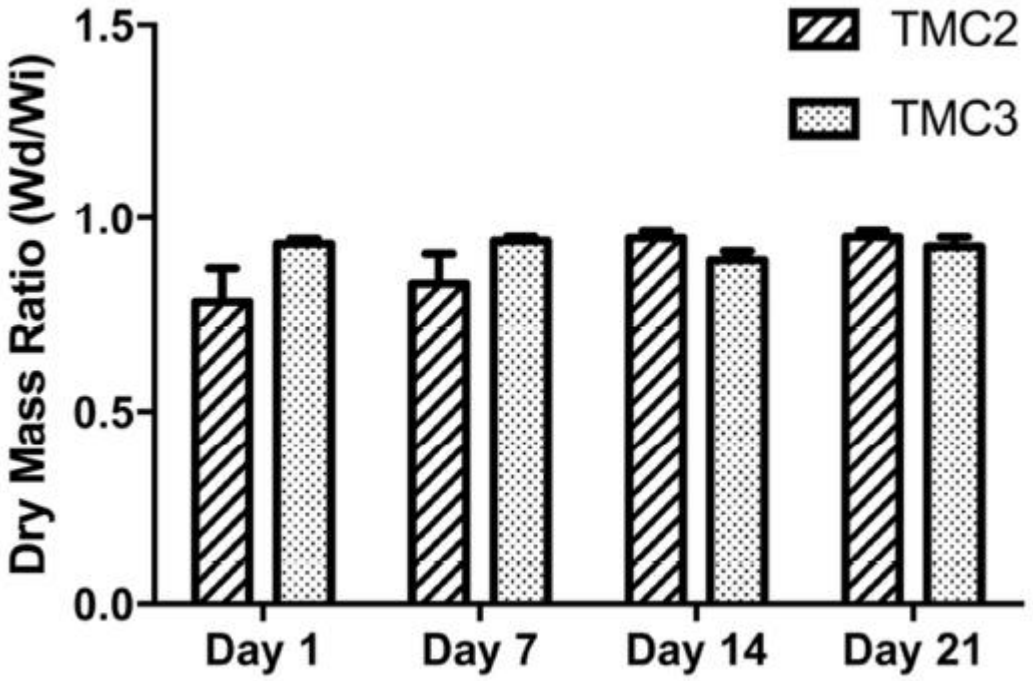

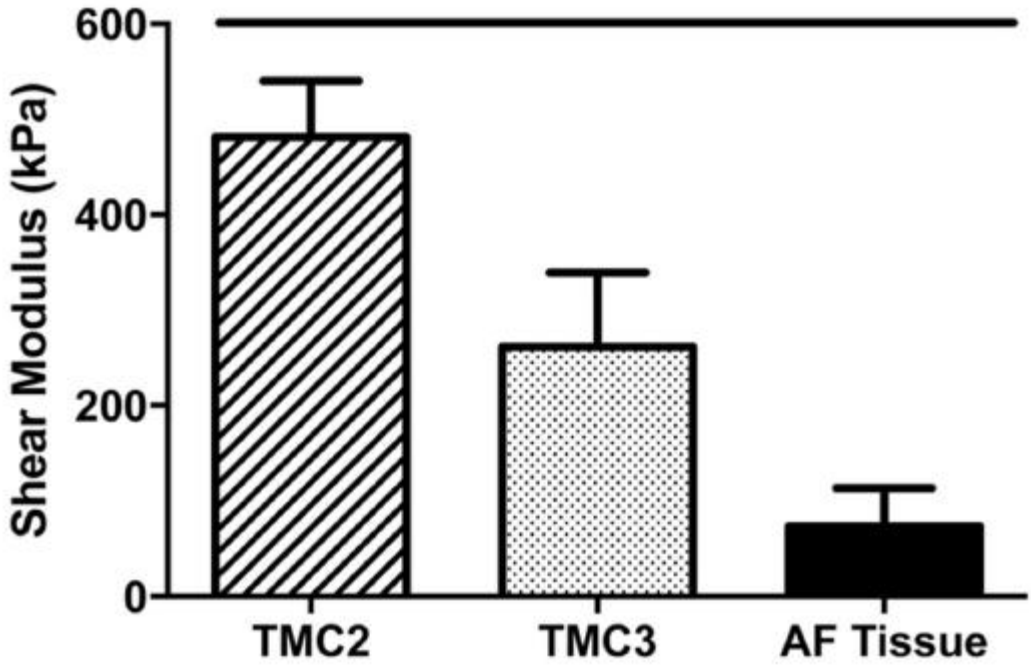

Figure 3. PEG based adhesives have high adhesion strength, low degradation rate and high shear modulus. (A) Both formulations of PEG-based adhesives, TMC2 and TMC3, had higher adhesion strength than the pressfit AF control. (B) The *swelling ratio* (Ww/Wd)~~*dry weight compared to the initial weight*~~ of both formulations remained constant through 3 weeks. ~~*TMC2 had a slight but statistically significant decrease within the first two weeks*~~. (C) The shear modulus of TMC2 was significantly greater than AF tissue (bar $p \leq 0.05$, letters indicate distinct statistical groups).

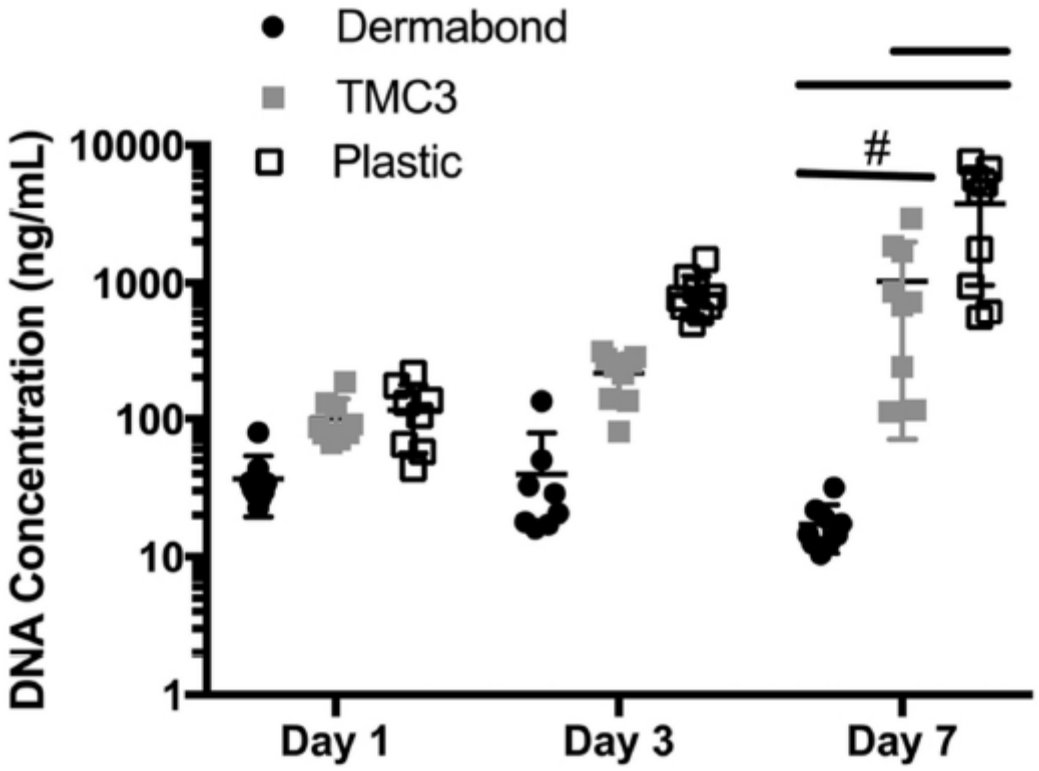

Figure 4. AF cells grow less rapidly on TMC3 and Dermabond than on tissue culture polystyrene (plastic). Cells grown on plastic had higher DNA concentration than cells grown on Dermabond and TMC3 at Day 7. Cells grown onTMC3 had a trend of higher DNA concentration than cells grown on Dermabond and tended to increase with time. Cells grown on plastic had higher DNA concentration at Day 7 than at Days 3 and 1 (* $p \leq 0.001$ from Day 3 and Day 1, bar $p \leq 0.05$, # $p \leq 0.10$).

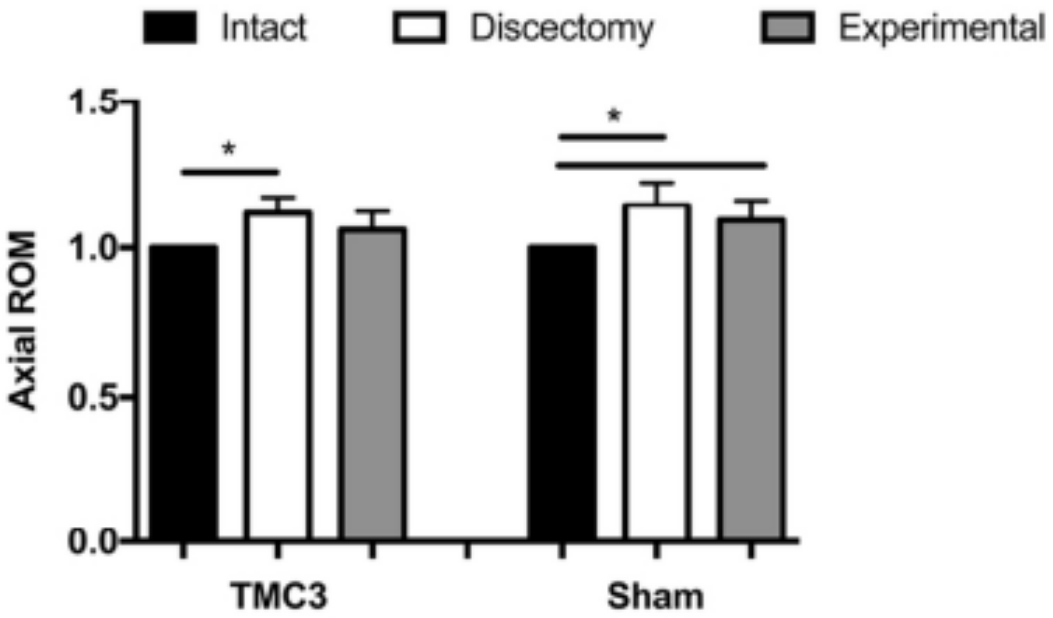

Figure 5. TMC3 partially restored in situ biomechanical behaviors to intact levels. Following discectomy. (A) Discectomy increased axial ROM and TMC3 repair restored to Intact condition. (B) Discectomy reduced torsion hysteresis area and TMC3 restored to Intact condition. (C) Discectomy reduced torsional stiffness and TMC3 repair restored to Intact condition. (D) Discectomy reduced torque range (bar $p \leq 0.05$,* $p \leq 0.01$). All parameters except torsional hysteresis were normalized to Intact condition.

Long.Fig6

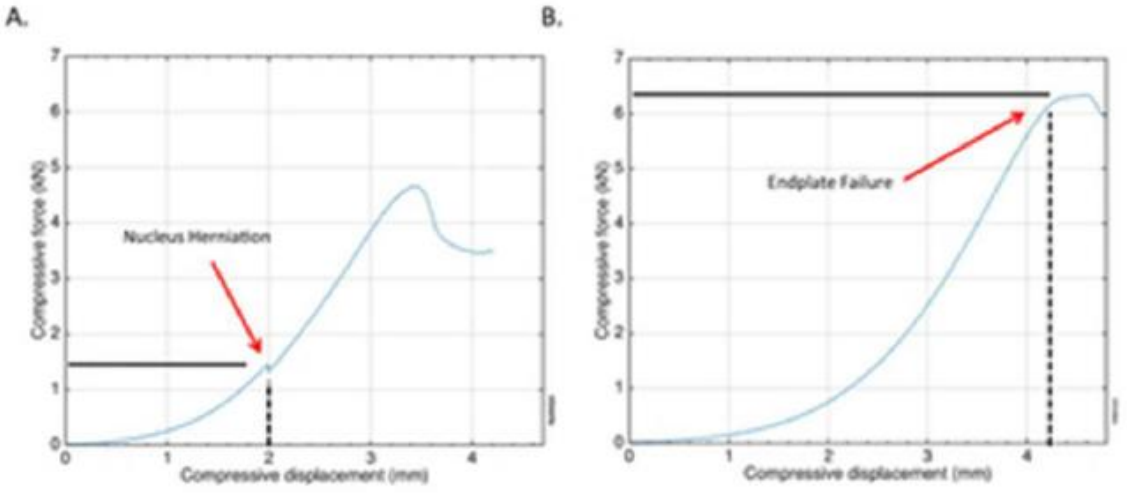

C.

Sample	Failure Strength (MPa)	Subsidence to failure (mm)	# failed by herniation
Intact	13.5 ± 4.2	3.30 ± 0.54	1/9
Discectomy	4.5 ± 2.7 *	2.09 ± 0.67 *	9/9
TMC3	5.9 ± 4.2 *	2.29 ± 0.69 *	9/9

Figure 6. TMC3 repaired samples failed at similar loads to non-repaired Discectomy samples. (A) One time loss of force in the force-displacement trace of a Discectomy sample indicated nucleus herniation. The solid line is the ultimate load, which is divided by cross-sectional area to get strength, and the dashed line is the subsidence to failure. (B) Gradual reduction in force of an Intact sample indicated endplate failure. (C) The TMC3 and Discectomy samples had similar failure strengths and subsidences that were lower than those of Intact samples (* $p \leq 0.05$). Failure was confirmed with video and dissection.

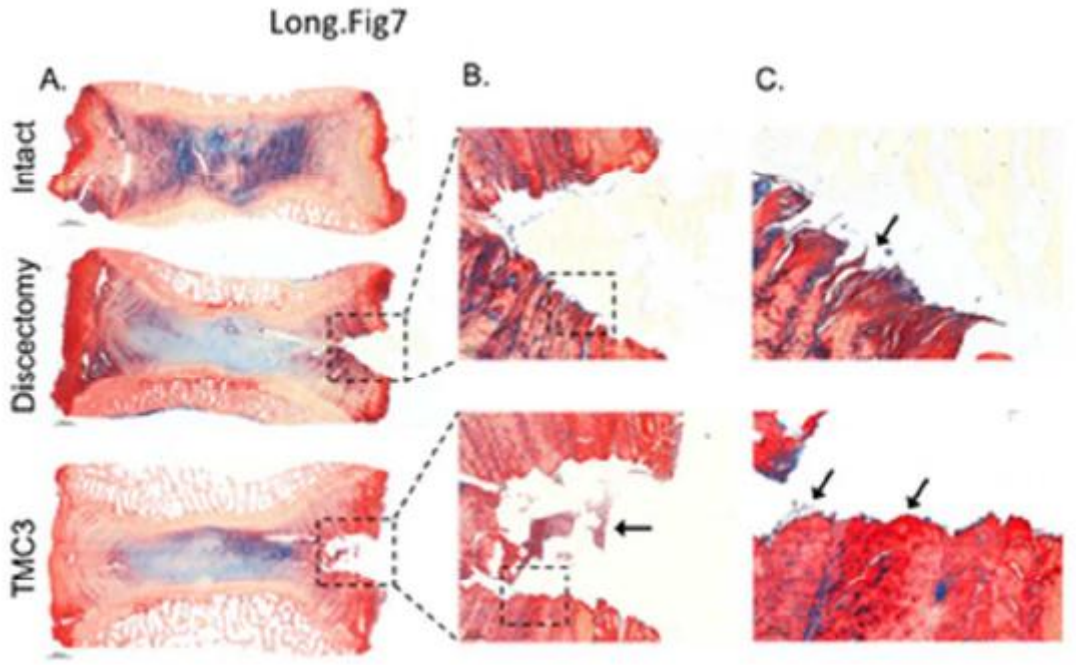

Figure 7. TMC3 better maintained IVD structure although expulsion occurred after cyclic loading. Pircosirius red/Alcian blue stained histological sections clearly demonstrated differences in (A) the overall structure of the IVD for intact, discectomy and TMC3 groups (bar 0.2 cm). (B) The TMC3 repair had a rectangular shaped defect where the TMC3 ‘plug’ was injected and expulsion of the TMC3 plug following cyclic loading dislodged some AF tissue (arrow). In contrast, the discectomy sample had a triangular shaped defect and more herniated NP material (bar 500 μm). (C) At AF defect surface, TMC3 maintained a smoother AF structure at the interface (arrow) while the discectomy group had a more disorganized AF structure at defect edge (arrow). Failure of the TMC3 repair predominantly occurred between AF tissue and TMC3, although some TMC3 remained adhered to the AF tissue (arrow; bar 200 μm).